Rational Design of a DNA Wire Possessing an Extremely High Hole Transport Ability

Akimitsu Okamoto, Kazuo Tanaka, and Isao Saito*

Contribution from the Department of Synthetic Chemistry and Biological Chemistry, Faculty of Engineering, Kyoto University, and SORST, Japan Science and Technology Corporation, Kyoto 606-8501, Japan

Received November 19, 2002; E-mail: saito@sbchem.kyoto-u.ac.jp

Abstract: DNA is a promising conductive biopolymer. However, there are problems that need to be solved to realize real DNA wires. These include the low efficiency of hole transport and the serious oxidative damage that can occur during hole transport. We have demonstrated a protocol for the design of a DNA wire that can effectively mediate hole transport that is not adversely affected by oxidation during hole transport through the DNA duplex. We have synthesized a stable and effective DNA wire by incorporating a designer nucleobase, benzodeazaadenine derivatives, which have lower oxidation potentials and wider stacking areas but are not decomposed during hole transport.

Introduction

In recent years, DNA has attracted much attention as a conductive biopolymer.[1] Recent efforts to elucidate the mechanism of long-range hole transport in DNA has encouraged us in the view that DNA can be a good mediator for hole transport by the selection of an appropriate sequence.[2] However, when natural DNA is used as a molecular wire, serious unavoidable oxidative degradation of G bases occurs. In addition, the hole transport in natural DNA is strongly influenced by the sequence and the transport distance.[2,3] Of great importance in the realization of a real DNA wire is the molecular design of an artificial nucleobase that can effectively mediate hole transport and, at the same time, is not oxidatively decomposed. We now report on a protocol for designing an artificial nucleobase that can act as an effective mediator for long-range hole transport without subsequent decomposition. By incorporating a designer nucleobase into DNA, we have accomplished an extremely effective hole transport between two GGG sites that are 76 Å apart without any detectable nucleobase decomposition.

Results and Discussion

We have designed an artificial nucleobase benzodeazaadenine (^{BD}A). This nucleobase would suppress the oxidative damage

caused by the addition of water and/or oxygen to the resulting radical cation (hole), which occurs in G runs,[4] and is expected to increase the hole transport efficiency because of the enhanced π-stacking arising from the expanded aromatic system. The synthesis of ^{BD}A nucleoside (**2**) was readily achieved in two steps from 4-chloro-1*H*-pyrimido[4,5-*b*]indole[5] as shown in Scheme 1, and **2** was incorporated via phosphoramidite **5** into DNA using a DNA synthesizer.

Initially, we examined the long-range hole transport through ^{BD}A-containing DNA to evaluate the hole transport efficiency and the degree of oxidative degradation of ^{BD}A. The method for determining the hole transport efficiency of the ^{BD}A-containing sequence is shown in Figure 1a. A hole was injected into duplex DNA by an electron-transfer reaction between cyanobenzophenone-substituted uridine (U*)[6] and an adjacent G by photoirradiation at 312 nm. Two GGG steps, which are known as an effective hole trap,[3,7] were incorporated into both sides of the sequence **I/II** separated by a T spacer. The hole transport efficiency of the sequence **I/II** was defined by the ratio of oxidative damage at the proximal (G_a) and distal GGG (G_b), as quantified by PAGE. The hole transport efficiency of ^{BD}A$_5$ (denoting five consecutive ^{BD}A units) as compared with those of related sequences is shown in Figure 1b. In the reaction of ^{BD}A$_5$, a reasonable hole transport value ($G_b/G_a = 0.36$) was observed, with no oxidative cleavage of ^{BD}A$_5$ even after a hot piperidine treatment. After photoirradiation, HPLC analysis of the enzyme-digested DNA showed no degradation of ^{BD}A (in contrast to G runs, where a 5% consumption of G was observed). In the G runs (i.e., G_5), the hole transport efficiency was

(1) (a) Fink, H.-W.; Schönenberger, C. *Nature* **1999**, *398*, 407−410. (b) Porath, D.; Bezryadin, A.; de Vries, S.; Dekker, C. *Nature* **2000**, *403*, 635−638. (c) Cai, L.; Tabata, H.; Kawai, T. *Appl. Phys. Lett.* **2000**, *77*, 3105−3106. (d) Kasumov, A. Y.; Kociak, M.; Guéron, S.; Reulet, B.; Volkov, V. T.; Klinov, D. V.; Bouchiat, H. *Science* **2001**, *291*, 280−281.

(2) (a) Hall, D. B.; Holmlin, R. E.; Barton, J. K. *Nature* **1996**, *382*, 731−735. (b) Burrows, C. J.; Muller, J. G. *Chem. Rev.* **1998**, *98*, 1109−1154. (c) Grinstaff, M. W. *Angew. Chem., Int. Ed.* **1999**, *38*, 3629−3635. (d) Núñez, M. E.; Barton, J. K. *Curr. Opin. Chem. Biol.* **2000**, *4*, 199−206. (e) Schuster, G. B. *Acc. Chem. Res.* **2000**, *33*, 253−260. (f) Giese, B. *Acc. Chem. Res.* **2000**, *33*, 631−636. (g) Lewis, F. D.; Letsinger, R. L.; Wasielewski, M. R. *Acc. Chem. Res.* **2001**, *34*, 159−170.

(3) Recently, A runs have been reported to be less distance-dependent mediators for hole transport. (a) Giese, B.; Amaudrut, J.; Köhler, A.-K.; Spormann, M.; Wessely, S. *Nature* **2001**, *412*, 318−320. (b) Kendrick, T.; Giese, B. *Chem. Commun.* **2002**, 2016−2017.

(4) Cadet, J.; Berger, M.; Buchko, G. W.; Joshi, P. C.; Raoul, S.; Ravanat, J.-L. *J. Am. Chem. Soc.* **1994**, *116*, 7403−7404.

(5) Showalter, H. D. H.; Bridges, A. J.; Zhou, H.; Sercel, A. D.; McMichael, A.; Fry, D. W. *J. Med. Chem.* **1999**, *42*, 5464−5474.

(6) Nakatani, K.; Dohno, C.; Saito, I. *J. Org. Chem.* **1999**, *64*, 6901−6904.

(7) Saito, I.; Nakamura, T.; Nakatani, K.; Yoshioka, Y.; Yamaguchi, K.; Sugiyama, H. *J. Am. Chem. Soc.* **1998**, *120*, 12686−12687.

Scheme 1[a]
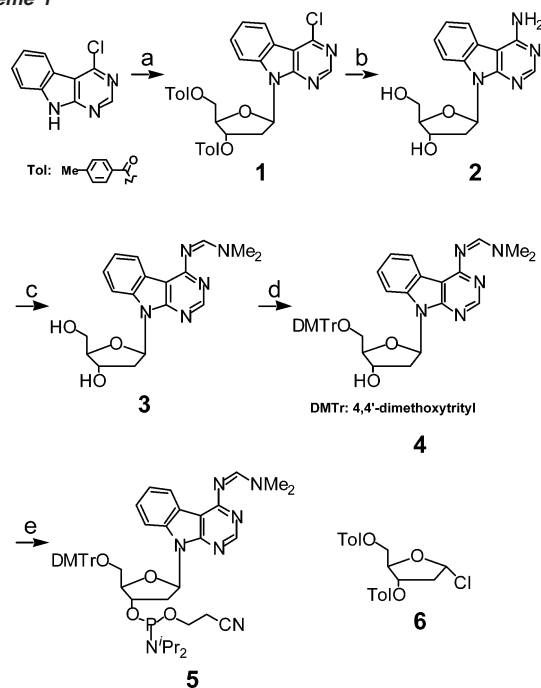
[a] (a) Sodium hydride, acetonitrile, room temperature, 91%; (b) methanolic ammonia, 150 °C, 72%; (c) DMF-dimethylacetal, DMF, 55 °C, 87%; (d) 4,4′-dimethoxytrityl chloride, pyridine, room temperature, 72%; (e) 2-cyanoethyl tetraisopropylphosphorodiamidite, tetrazole, acetonitrile, room temperaure, quant.
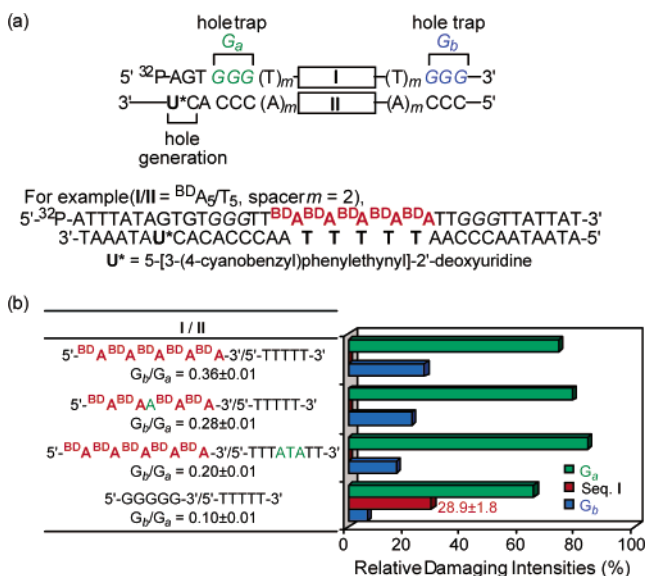

Figure 1. (a) A DNA sequence for measuring the hole transport efficiency of sequence **I/II**. (b) The ratio G_b/G_a of oxidative damage at G_a and G_b, and the damaging intensity at hole-transporting sequence **I/II**. The duplexes (spacer $m = 2$) in 10 mM sodium cacodylate (pH 7.0) were irradiated ($\lambda = 312$ nm) at 0 °C for 45 min followed by a hot piperidine treatment. The relative damaging intensities show the percentage of strand breakages at G_a, G_b, and sequence **I** relative to the total strand cleavage obtained by densitometric analysis. The hole-trapping ratio (G_b/G_a) corresponding to the hole transport efficiency of sequence **I/II** was calculated from the relative intensities of the oxidative cleavage bands at G_a and G_b.

relatively low ($G_b/G_a = 0.10$), and the DNA was strongly damaged at the G_5 site. In the reaction of a sequence where the central ^{BD}A unit of the $^{BD}A_5$ run was replaced by A separating the ^{BD}A units, and for a sequence where an ATA 3-base bulge[8] was inserted, the G_b/G_a damaging ratios decreased to 0.28 and
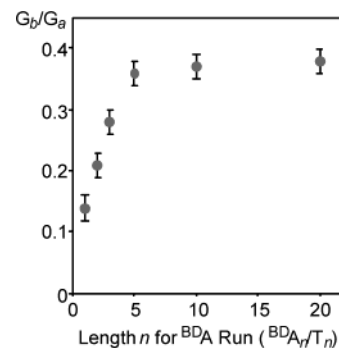

Figure 2. Correlation of the hole transport efficiency to the length of the ^{BD}A runs (spacer $m = 2$). Estimated error for G_b/G_a was ±0.02.
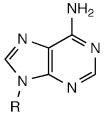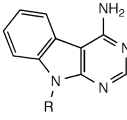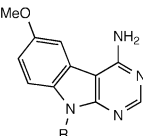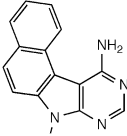
0.20, respectively. This showed that the hole transport efficiency decreases by breaking the stacking between the ^{BD}A units. These results imply that a stack of ^{BD}A runs can provide a high hole transport efficiency. It is also noteworthy that the length of the spacer separating the sequence **I/II** and the GGG hole trap also affected the G_b/G_a damaging ratio.[2f] When the spacer length, m, was changed from 2 to 1, the G_b/G_a damaging ratio greatly increased to 0.78 ± 0.06, suggesting that $^{BD}A_5$ is inherently a very effective hole transport mediator.

We next investigated the efficiency of hole transport through the ^{BD}A runs, by increasing the number (n) of ^{BD}A runs from 1 to 20 to know the effect of the length of the π-stacking array of the ^{BD}A runs on the hole transport efficiency. Figure 2 shows the resulting G_b/G_a damaging ratio plotted against n. The G_b/G_a ratio increased with an increasing number of ^{BD}A units in the $^{BD}A_n$ runs (for $n = 1-5$). This result is in sharp contrast to the hole transport behavior generally observed in natural DNA, which drops off rapidly with increasing distance.[9] Furthermore, G_b/G_a became saturated at a value of ca. 0.4, when the number of ^{BD}A units was greater than five. It has been proposed that stationary polarons in DNA can extend over 5−7 base pairs,[2e,10] and, hence, the influence of the length of the ^{BD}A runs on the hole transport efficiency would possibly relate to the polaron width generated in the DNA. PAGE analysis of these reactions did not show any oxidative degradation of ^{BD}A, regardless of the number of ^{BD}A units in the ^{BD}A runs. Such an effective long-range hole transport without any degradation of the G units is very difficult to achieve in natural DNA.

We next prepared two ^{BD}A derivatives, methoxy-substituted ^{MD}A and naphthalene-fused NDA, to elucidate the influence of the oxidation potential and the stacking surface area on the hole transport efficiency. Both the ionization potential[11] and the base stacking[3,12] of the bridge sequence have been discussed as important factors for hole transport efficiency through DNA. The synthesis of ^{MD}A-containing DNA was readily achieved from 4-chloro-6-methoxy-1H-pyrimido[4,5-b]indole[5] as shown

(8) Rosen, M. A.; Shapiro, L.; Patel, D. J. *Biochemistry* **1992**, *31*, 4015−4026.
(9) (a) Bixon, M.; Giese, B.; Wessely, S.; Langenbacher, T.; Michel-Beyerle, M. E.; Jortner, J. *Proc. Natl. Acad. Sci. U.S.A.* **1999**, *96*, 11713−11716. (b) Grozema, F. C.; Berlin, Y. A.; Siebbeles, L. D. A. *J. Am. Chem. Soc.* **2000**, *122*, 10903−10909.
(10) (a) Conwell, E. M.; Rakhmanova, S. V. *Proc. Natl. Acad. Sci. U.S.A.* **2000**, *97*, 4556−4560. (b) Rakhmanova, S. V.; Conwell, E. M. *J. Phys. Chem. B* **2001**, *105*, 2056−2061.
(11) (a) Saito, I.; Nakamura, T.; Nakatani, K.; Yoshioka, Y.; Yamaguchi, K.; Sugiyama, H. *J. Am. Chem. Soc.* **1998**, *120*, 12686−12687. (b) Nakatani, K.; Dohno, C.; Saito, I. *J. Am. Chem. Soc.* **2000**, *122*, 5893−5894.
(12) (a) Holmlin, R. E.; Dandliker, P. J.; Barton, J. K. *Angew. Chem., Int. Ed. Engl.* **1997**, *24*, 2715−2730. (b) Treadway, C. R.; Hill, M. G.; Barton, J. K. *Chem. Phys.* **2002**, *281*, 409−428.

Table 1. Hole Transport Efficiencies (G_b/G_a) of Adenine and ^{BD}A Analogues

Bases (**X**)				
	A	^{BD}**A**	^{MD}**A**	ND**A**
Oxidation Potential $(E_p)^a$	1.45 V	1.32 V	1.10 V	1.03 V
Stacking Surface Area^b	137.1 Å^2	160.1 Å^2	188.3 Å^2	194.7 Å^2
G_b/G_a (**I/II = X/T**)	~0	0.14±0.02	0.43±0.04	0.50±0.05
G_b/G_a (**I/II = X$_2$/T$_2$**)	——^{c}	0.21±0.02	0.67±0.05	0.53±0.08

^{a} Oxidation potentials (E_p, vs SCE) of nucleosides (R = 2′-deoxyribos-1′-yl) were obtained from cyclic voltammograms. The E_p of G was 1.15 V. ^{b} The stacking surface area of **X$_2$/T$_2$** (R = H) was calculated by AMBER* (water set) in MacroModel 6.0. ^{c} Experiment was not carried out.

Scheme 2 ^{a}
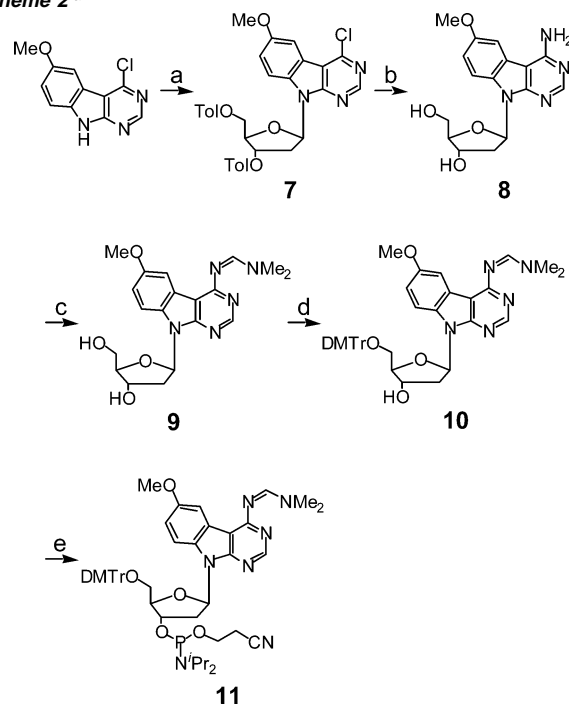
^{a} (a) Sodium hydride, acetonitrile, room temperature, 82%; (b) methanolic ammonia, 150 °C, 75%; (c) DMF-dimethylacetal, DMF, 60 °C, 88%; (d) 4,4′-dimethoxytrityl chloride, pyridine, room temperature, 75%; (e) 2-cyanoethyl tetraisopropylphosphorodiamidite, tetrazole, acetonitrile, room temperature, quant.

Figure 3. Effective hole transport through an ^{MD}A run. (a) The sequence of duplex DNA containing ^{MD}A$_{20}$/T$_{20}$. (b) An autoradiogram of a denaturing gel electrophoresis of ^{32}P-5′-end-labeled DNA after photoirradiation of the duplex. Lane 1, Maxam−Gilbert G + A sequencing lane; lane 2, control lane (no photoirradiation); lane 3, duplex DNA photoirradiated as described in Figure 1. (c) Densitometric analysis of lane 3 of Figure 3b. The G_b/G_a ratio obtained from the peak areas of the cleavage bands at both GGG sites was 0.99 ± 0.04.

in Scheme 2. The G_b/G_a damaging ratios for ^{MD}A and ^{MD}A$_2$ were 0.43 and 0.67, respectively, showing a remarkable increase in the hole transport efficiency (Table 1). In addition, in NDA, the hole transport efficiency was higher than that observed for ^{BD}A. Both ^{MD}A and NDA had lower oxidation potentials than that of ^{BD}A, and the stacking surface areas of dimers ^{MD}A$_2$/T$_2$ and NDA$_2$/T$_2$ obtained from the calculation of the water-accessible surface were enhanced by 18 and 22%, respectively, when compared to that calculated for ^{BD}A. These results indicate that both the oxidation potential and the stacking of the nucleobases play a key role in mediating a hole transport.

On the basis of these results, we designed a DNA sequence containing ^{MD}A$_{20}$ and investigated the hole transport efficiency. As shown in Figure 3, the G_b/G_a damaging ratio was 0.99 ± 0.04, implying that a hole in the DNA was effectively free to
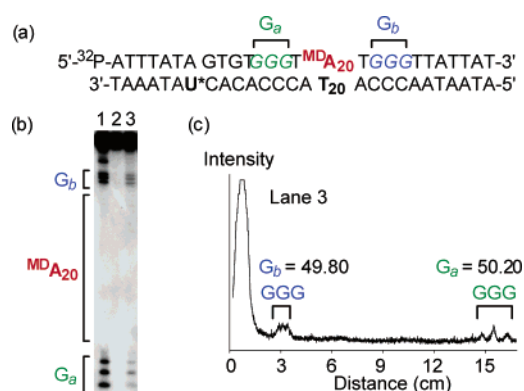
migrate between two GGG sites (a distance of ca. 7.6 nm). Although ^{MD}A has a smaller oxidation potential than G, no damage of the ^{MD}A$_{20}$ was observed from either PAGE analysis or HPLC analysis after enzyme digestion of photoirradiated DNA. HPLC analysis for the enzyme-digested DNA after photoirradiation showed 7% destruction of G with almost no ^{MD}A decomposition (see Supporting Information). This is quite different from the behavior seen in the G runs. As is needed for a molecular wire, the ^{MD}A run behaved as a good mediator for hole transport and was not oxidatively decomposed.

Conclusions

In conclusion, we have demonstrated a protocol for building a DNA nanowire. We indicated three important factors that are prerequisites for designing real DNA nanowires: (i) a highly ordered π-stacking array, (ii) low oxidation potentials, and (iii) suppressed oxidative degradation. In particular, the ^{MD}A runs developed according to this principle showed a remarkably high hole transport ability, similar to that expected for a molecular wire. These DNA wires are suitable for further development encompassing site-specific fabrication and functionalization, which are difficult and troublesome for known conductive materials, such as carbon nanotubes and conductive polymers. In addition, they are expected to constitute a new, well-regulated

bionanomaterial that will be widely applicable to electronic devices and biosensors.

Experimental Section

General. ^{1}H NMR spectra were measured with Varian Mercury 400 (400 MHz) spectrometer. ^{13}C NMR spectra were measured with JEOL JNM a-500 (500 MHz) spectrometer. Coupling constants (*J* value) are reported in hertz. The chemical shifts are expressed in ppm downfield from tetramethylsilane, using residual chloroform ($\delta = 7.24$ in ^{1}H NMR, $\delta = 77.0$ in ^{13}C NMR) and dimethyl sulfoxide ($\delta = 2.48$ in ^{1}H NMR, $\delta = 39.5$ in ^{13}C NMR) as an internal standard. FAB mass spectra were recorded on a JEOL JMS DX-300 spectrometer or JEOL JMS SX-102A spectrometer. HPLC was performed on a Cosmosil 5C-18AR or CHEMCOBOND 5-ODS-H column (4.6 × 150 mm) with a Gilson chromatography model 305 using a UV detector model 118 at 254 nm.

4-Chloro-7-(2-deoxy-3,5-di-*O*-*p*-toluoyl-β-D-*erythro*-pentofuranosyl)-7*H*-pyrimido[4,5-*b*]indole (1). 4-Chloro-1*H*-pyrimido[4,5-*b*]indole (360 mg, 1.77 mmol) was suspended in dry acetonitrile (250 mL) at ambient temperature. To this suspension was added sodium hydride (60% in oil; 142 mg, 3.54 mmol), and the mixture was stirred at reflux for 10 min. The ribose **6** (687 mg, 1.77 mmol) was added, and the mixture was stirred for 1 h at ambient temperature. The reaction mixture was concentrated and purified by column chromatography on silica gel, eluting with 20% ethyl acetate in hexane to give compound **1** (890 mg, 91%). ^{1}H NMR (CDCl$_3$): δ 8.71 (s, 1H), 8.36 (d, 1H, *J* = 7.9 Hz), 7.99 (d, 2H, *J* = 8.2 Hz), 7.95 (d, 2H, *J* = 6.6 Hz), 7.79 (d, 1H, *J* = 8.4 Hz), 7.37 (dt, 1H, *J* = 8.1, 0.7 Hz), 7.28 (d, 2H, *J* = 8.1 Hz), 7.27 (dt, 1H, *J* = 8.2, 1.1 Hz), 7.23 (d, 2H, *J* = 8.4 Hz), 7.03 (dd, 1H, *J* = 8.8, 6.2 Hz), 5.93 (dt, 1H, *J* = 6.2, 2.7 Hz), 4.86 (dd, 2H, *J* = 11.1, 3.5 Hz), 4.59 (dd, 1H, *J* = 7.2, 3.9 Hz), 3.56 (ddd, 1H, *J* = 16.1, 7.5, 7.2 Hz), 2.59 (ddd, 1H, *J* = 14.4, 6.2, 2.4 Hz), 2.43 (s, 3H), 2.41 (s, 3H). ^{13}C NMR (CDCl$_3$): δ 166.2, 166.1, 155.6, 153.5, 152.7, 144.4, 144.0, 137.8, 129.8, 129.7, 129.3, 129.2, 128.3, 126.9, 126.5, 123.4, 122.6, 119.1, 112.8, 112.1, 83.6, 81.8, 74.4, 63.8, 35.3, 21.73, 21.70. MS (FAB, NBA/CH$_2$Cl$_2$): *m/z* (%) 556 [(M + H)$^+$]. HRMS (FAB) calcd for C$_{31}$H$_{27}$ClN$_3$O$_7$ [(M + H)$^+$] 556.1639, found 556.1638.

4-Amino-9-(2′-deoxy-β-D-*erythro*-pentofuranosyl)-7*H*-pyrimido-[4,5-*b*]indole (2, ^{BD}A). A suspension of **1** (300 mg, 0.54 mmol) in 20 mL of methanolic ammonia (saturated at −76 °C) was stirred at 150 °C in a sealed bottle for 10 h. The turbid solution was concentrated and purified by column chromatography on silica gel, eluting with 10% methanol in chloroform to give compound **2** (117 mg, 72%). ^{1}H NMR (DMSO-*d$_6$*): δ 8.31 (d, 1H, *J* = 7.7 Hz), 8.27 (s, 1H), 7.84 (d, 1H, *J* = 8.2 Hz), 7.37 (dt, 1H, *J* = 8.2, 1.1 Hz), 7.32−7.25 (3H), 6.82 (dd, 1H, *J* = 8.8, 6.0 Hz), 5.32 (d, 1H, *J* = 4.4 Hz), 5.28 (t, 1H, *J* = 4.9 Hz), 4.46 (m, 1H), 3.86 (dd, 1H, *J* = 7.3, 3.8 Hz), 3.66 (m, 2H), 2.88 (ddd, 1H, *J* = 15.6, 8.8, 6.6 Hz), 2.05 (ddd, 1H, *J* = 15.4, 6.0, 2.2 Hz). ^{13}C NMR (DMSO-*d$_6$*): δ 157.7, 154.7, 154.4, 135.5, 124.7, 121.3, 121.0, 120.2, 111.8, 87.1, 82.8, 70.9, 61.9, 37.5, 31.5. MS (FAB, NBA/DMSO): *m/z* (%) 301 [(M + H)$^+$]. HRMS (FAB) calcd for C$_{15}$H$_{17}$N$_4$O$_3$ [(M + H)$^+$] 301.1301, found 301.1297.

4-(*N,N′*-Dimethylaminomethylidene)amino-9-(2′-deoxy-β-D-*erythro*-pentofuranosyl)-9*H*-pyrimido[4,5-*b*]indole (3). A solution of **2** (130 mg, 0.43 mmol) and *N,N*-dimethylformamide dimethylacetal (5 mL, 28.3 mmol) in *N,N*-dimethylformamide (5 mL) was stirred for 18 h at 55 °C. The reaction mixture was concentrated to a brown oil and purified by column chromatography on silica gel, eluting with 10% methanol in chloroform to give compound **3** (134 mg, 87%). ^{1}H NMR (CDCl$_3$): δ 8.94 (s, 1H), 8.53 (s, 1H), 8.41 (d, 1H, *J* = 7.1 Hz), 7.49 (d, 1H, *J* = 8.1 Hz), 7.44 (dt, 1H, *J* = 7.1, 1.1 Hz), 7.30 (dt, 1H, *J* = 7.8, 0.9 Hz), 6.73 (dd, 1H, *J* = 8.9, 5.5 Hz), 4.83 (d, 1H, *J* = 5.1 Hz), 4.23 (s, 1H), 4.01 (dd, 1H, *J* = 2.9, 1.4 Hz), 3.82 (m, 1H), 3.31 (s, 3H), 3.29−3.22 (m, 2H), 3.21 (s, 3H), 2.23 (dd, 2H, *J* = 15.4, 5.7 Hz). ^{13}C NMR (CDCl$_3$): δ 161.9, 156.8, 155.2, 153.1, 137.9, 125.9,

123.7, 121.4, 121.0, 108.9, 88.8, 85.7, 74.0, 63.8, 41.2, 39.9, 35.2, 31.4. MS (FAB, NBA/CH$_2$Cl$_2$): *m/z* (%) 356 [(M + H)$^+$]. HRMS (FAB) calcd for C$_{18}$H$_{22}$N$_5$O$_3$ [(M + H)$^+$] 356.1723, found 356.1722.

4-(*N,N′*-Dimethylaminomethylidene)amino-9-(2′-deoxy-5′-*O*-dimethoxytrityl-β-D-*erythro*-pentofuranosyl)-9*H*-pyrimido[4,5-*b*]-indole (4). A solution of **3** (60 mg, 0.18 mmol) and 4,4′-dimethoxytrityl chloride (8.0 mg, 0.24 mmol) was stirred in anhydrous pyridine (10 mL) for 2 h at ambient temperature. The reaction mixture was concentrated to a brown oil and purified by column chromatography on silica gel, eluting with a mixed solution of 50:50:5 (v/v/v) hexane, ethyl acetate, and triethylamine to give compound **4** (80 mg, 72%). ^{1}H NMR (CDCl$_3$): δ 8.91 (s, 1H), 8.53 (s, 1H), 8.39 (d, 1H, *J* = 7.7 Hz), 7.70 (d, 1H, *J* = 8.3 Hz), 7.43 (dd, 2H, *J* = 8.6, 1.5 Hz), 7.31 (dd, 4H, *J* = 9.0, 1.5 Hz), 7.27−7.13 (5H), 6.94 (t, 1H, *J* = 7.3 Hz), 6.75 (dt, 4H, *J* = 9.9, 3.1 Hz), 4.85 (dt, 1H, *J* = 7.7, 4.4 Hz), 4.04 (q, 1H, *J* = 4.6 Hz), 3.747 (s, 3H), 3.745 (s, 3H), 3.48 (d, 1H, *J* = 4.6 Hz), 3.30 (s, 3H), 3.21 (s, 3H), 3.25−3.19 (m, 1H), 2.29 (ddd, 1H, *J* = 13.7, 7.0, 3.8 Hz). ^{13}C NMR (CDCl$_3$): δ 161.3, 158.4, 156.52, 156.47, 154.0, 144.7, 136.8, 135.8, 130.14, 130.11, 128.2, 127.8, 126.8, 125.6, 123.5, 121.8, 121.4, 113.1, 111.7, 105.6, 86.5, 84.5, 82.7, 72.6, 63.6, 60.4, 55.2, 45.6, 41.0, 37.7, 35.1, 21.1, 14.2. MS (FAB, NBA/CH$_2$Cl$_2$): *m/z* (%) 658 [(M + H)$^+$]. HRMS (FAB) calcd for C$_{39}$H$_{40}$N$_5$O$_5$ [(M + H)$^+$] 658.2951, found 658.3038.

4-(*N,N′*-Dimethylaminomethylidene)amino-9-(2′-deoxy-5′-*O*-dimethoxytrityl-β-D-*erythro*-pentofuranosyl-3′-*O*-cyanoethyl-*N,N′*-diisopropylphosphoramidite)-9*H*-pyrimido[4,5-*b*]indole (5). A solution of **4** (10 mg, 15.2 μmol), 2-cyanoethyl tetraisopropylphosphorodiamidite (5.3 μL, 16.7 mmol), and tetrazole (1.2 mg, 16.7 mmol) in acetonitrile (400 μL) was stirred at ambient temperature for 2 h. The mixture was filtered off and used without further purification.

4-Chloro-6-methoxy-7-(2-deoxy-3,5-di-*O*-*p*-toluoyl-β-D-*erythro*-pentofuranosyl)-7*H*-pyrimido[4,5-*b*]indole (7). 4-Chloro-6-methoxy-1*H*-pyrimido[4,5-*b*]indole (100 mg, 0.43 mmol) was suspended in dry acetonitrile (10 mL) at ambient temperature. To this suspension was added sodium hydride (60% in oil; 19 mg, 0.47 mmol), and the mixture was stirred at reflux for 10 min. The ribose **6** (184 mg, 0.47 mmol) was added, and the mixture was stirred for 1 h at ambient temperature. The reaction mixture was concentrated and purified by column chromatography on silica gel, eluting with 20% ethyl acetate in hexane to give compound **7** (210 mg, 82%). ^{1}H NMR (CDCl$_3$): δ 8.69 (s, 1H), 7.97 (d, 2H, *J* = 14.8 Hz), 7.96 (d, 2H, *J* = 14.8 Hz), 7.82 (d, 1H, *J* = 2.6 Hz), 7.68 (d, 1H, *J* = 4.0 Hz), 7.27 (d, 2H, *J* = 16.8 Hz), 7.24 (d, 2H, *J* = 15.7 Hz), 7.00 (dd, 1H, *J* = 8.8, 6.1 Hz), 6.82 (dd, 1H, *J* = 9.0, 2.6 Hz), 5.90 (dt, 1H, *J* = 7.0, 3.3 Hz), 4.85 (dd, 1H, *J* = 12.1, 3.3 Hz), 4.70 (dd, 1H, *J* = 12.1, 4.0 Hz), 4.57 (dt, 1H, *J* = 7.1, 3.6 Hz), 3.87 (s, 3H), 3.48 (ddd, 1H, *J* = 16.3, 8.8, 5.7 Hz), 2.57 (ddd, 1H, *J* = 14.3, 6.0, 2.9 Hz), 2.43 (s, 3H), 2.41 (s, 3H). ^{13}C NMR (CDCl$_3$): δ 166.2, 166.1, 155.8, 155.7, 153.4, 152.7, 144.4, 144.0, 132.2, 129.8, 129.7, 129.3, 129.2, 126.9, 126.5, 119.9, 117.1, 113.0, 112.7, 106.1, 83.6, 81.7, 74.4, 63.8, 55.9, 35.4, 21.74, 21.71. MS (FAB, NBA/CH$_2$Cl$_2$): *m/z* (%) 634 [(M + H)$^+$]. HRMS (FAB) calcd for C$_{32}$H$_{29}$ClN$_3$O$_8$ [(M + H)$^+$] 634.2552, found 634.2553.

4-Amino-6-methoxy-9-(2′-deoxy-β-D-*erythro*-pentofuranosyl)-7*H*-pyrimido[4,5-*b*]indole (8, ^{MD}A). A suspension of **7** (500 mg, 0.85 mmol) in 20 mL of methanolic ammonia (saturated at −76 °C) was stirred at 150 °C in a sealed bottle for 10 h. The turbid solution was concentrated and purified by column chromatography on silica gel, eluting with 10% methanol in chloroform to give compound **8** (420 mg, 75%). ^{1}H NMR (DMSO-*d$_6$*): δ 8.23 (s, 1H), 7.86 (d, 1H, *J* = 2.4 Hz), 7.73 (d, 1H, *J* = 8.8 Hz), 7.29 (br, 2H), 6.97 (dd, 1H, *J* = 9.0, 2.6 Hz), 6.78 (dd, 1H, *J* = 9.0, 6.2 Hz), 5.26 (d, 1H, *J* = 4.4 Hz), 5.20 (t, 1H, *J* = 5.8 Hz), 4.43 (m, 1H), 3.85 (s, 3H), 3.65 (m, 2H), 3.27 (s, 3H), 2.82 (ddd, 1H, *J* = 13.0, 6.8, 2.8 Hz), 2.01 (ddd, 1H, *J* = 13.1, 6.2, 2.3 Hz). ^{13}C NMR (DMSO-*d$_6$*): δ 157.6, 154.8, 154.7, 154.3, 129.9, 120.8, 113.0, 112.4, 104.9, 95.6, 86.9, 82.7, 70.8, 61.8, 55.9, 37.4. MS

(FAB, NBA): m/z (%) 331 [(M + H)$^+$]. HRMS (FAB) calcd for $C_{16}H_{19}N_4O_4$ [(M + H)$^+$] 331.1406, found 331.1402.

4-(N,N'-Dimethylaminomethylidene)amino-6-methoxy-9-(2′-deoxy-β-D-*erythro*-pentofuranosyl)-9H-pyrimido[4,5-*b*]indole (9). A solution of **8** (90 mg, 0.27 mmol) and N,N-dimethylformamide dimethylacetal (10 mL) in N,N-dimethylformamide (10 mL) was stirred for 3 h at 60 °C. The reaction mixture was concentrated to a brown oil and purified by column chromatography on silica gel, eluting with 10% methanol in chloroform to give compound **9** (120 mg, 88%). ^{1}H NMR (CDCl$_3$): δ 8.93 (s, 1H), 8.50 (s, 1H), 7.97 (d, 1H, J = 2.8 Hz), 7.39 (d, 1H, J = 9.0 Hz), 7.06 (dd, 1H, J = 8.8, 2.6 Hz), 6.66 (dd, 1H, J = 9.9, 5.5 Hz), 4.82 (d, 1H, J = 4.9 Hz), 4.22 (s, 1H), 4.02 (d, 1H, J = 1.6 Hz), 3.90 (s, 3H), 3.82 (m, 1H), 3.31 (s, 3H), 3.22 (s, 3H), 2.94 (s, 1H), 2.86 (s, 1H), 2.21 (dd, 1H, J = 13.5, 5.7 Hz). ^{13}C NMR (CDCl$_3$): δ 161.8, 156.8, 155.3, 155.0, 153.1, 132.6, 121.7, 114.3, 109.6, 107.1, 106.8, 88.8, 85.9, 74.0, 63.8, 55.8, 41.2, 39.4, 35.1. MS (FAB, NBA/CH$_2$Cl$_2$): m/z (%) 386 [(M + H)$^+$]. HRMS (FAB) calcd for $C_{19}H_{24}N_5O_4$ [(M + H)$^+$] 386.1828, found 386.1827.

4-(N,N'-Dimethylaminomethylidene)amino-6-methoxy-9-(2′-deoxy-5′-*O*-dimethoxytrityl-β-D-*erythro*-pentofuranosyl)-9H-pyrimido[4,5-*b*]indole (10). A solution of **9** (120 mg, 0.1 mmol) and 4,4′-dimethoxytrityl chloride (137.0 mg, 0.41 mmol) was stirred in anhydrous pyridine (10 mL) for 2 h at ambient temperature. The reaction mixture was concentrated to a brown oil and purified by column chromatography on silica gel, eluting with a mixed solution of 90:3:5 (v/v/v) chloroform, methanol, and triethylamine to give compound **10** (161 mg, 75%). ^{1}H NMR (CDCl$_3$): δ 8.89 (s, 1H), 8.50 (s, 1H), 7.94 (dt, 1H, J = 2.9, 2.2 Hz), 7.62 (d, 1H, J = 9.0 Hz), 7.31 (dd, 2H, J = 8.8, 1.9 Hz), 7.25−7.15 (8H), 6.94 (t, 1H, J = 5.3 Hz), 6.75 (d, 4H, J = 8.6 Hz), 6.68 (dd, 2H, J = 6.9, 2.7 Hz), 4.84−4.80 (m, 1H), 4.05 (q, 1H, J = 4.4 Hz), 3.83 (s, 3H), 3.76 (s, 3H), 3.48 (d, 2H, J = 4.4 Hz), 3.28 (s, 3H), 3.19 (s, 3H), 3.16−3.11 (m, 1H), 2.93 (dt, 1H, J = 14.2, 6.9 Hz), 2.27 (ddd, 1H, J = 13.5, 6.8, 3.5 Hz). ^{13}C NMR (CDCl$_3$): δ 161.3, 158.5, 156.6, 156.5, 155.0, 153.9, 144.7, 135.8, 135.76, 131.4, 130.17, 130.14, 129.8, 129.1, 128.2, 127.8, 126.8, 122.6, 113.7, 113.1, 112.6, 107.0, 105.6, 86.5, 84.6, 82.7, 72.4, 63.5, 55.2, 45.5, 41.0, 37.8, 35.0, 9.0. MS (FAB, NBA/CH$_2$Cl$_2$): m/z (%) 688 [(M + H)$^+$]. HRMS (FAB) calcd for $C_{40}H_{42}N_5O_6$ [(M + H)$^+$] 688.3135, found 688.3134.

4-(N,N'-Dimethylaminomethylidene)amino-6-methoxy-9-(2′-deoxy-5′-*O*-dimethoxytrityl-β-D-*erythro*-pentofuranosyl-3′-*O*-cyanoethyl-N,N'-diisopropylphosphoramidite)-9H-pyrimido[4,5-*b*]indole (11). A solution of **10** (50 mg, 72.7 μmol), 2-cyanoethyl tetraisopropylphosphorodiamidite (25 μL, 79.9 μmol), and tetrazole (7 mg, 0.1 mmol) in acetonitrile (500 μL) was stirred at ambient temperature for 2 h. The mixture was filtered and used without further purification.

Modified ODN Synthesis. Modified ODNs were synthesized by the conventional phosphoramidite method using an Applied Biosystems 392 DNA/RNA synthesizer. Synthesized ODNs were purified by reversed phase HPLC on a 5-ODS-H column (10 × 150 mm, elution with a solvent mixture of 0.1 M triethylammonium acetate (TEAA), pH 7.0, linear gradient over 30 min from 5 to 20% acetonitrile at a flow rate 3.0 mL/min) or 15% denaturing polyacrylamide gel electrophoresis (PAGE). Mass spectra of ODNs purified by HPLC were determined with ESI-TOF mass spectroscopy or MALDI-TOF mass spectroscopy (acceleration voltage 21 kV, negative mode) with 2′,3′,4′-trihydroxyacetophenone as matrix, using T_8 ([M − H]$^-$ 2370.61) and T_{17} ([M − H]$^-$ 5108.37) as an internal standard. The ODNs purified by PAGE were characterized by Maxam−Gilbert sequencing reactions.

5′-d(ATTTATAGTGTGGGTT^{BD}A^{BD}A^{BD}A^{BD}A^{BD}ATTGGGTTATTAT)-3′: MALDI-TOF [(M − H)$^-$] calcd 10 511.00, found 10 511.80. 5′-d(ATTTATAGTGTGGGTT^{BD}A^{BD}AA^{BD}A^{BD}ATTGGGTTATTAT)-3′: MALDI-TOF [(M − H)$^-$] calcd 10 461.93, found 10 461.20. 5′-d(ATTTATAGTGTGGGT^{BD}A^{BD}A^{BD}A^{BD}A^{BD}ATGGGTTATTAT)-3′: MALDI-TOF [(M − H)$^-$] calcd 9901.61, found 9903.96. 5′-d(ATTTATA-

GTGTGGGTT^{BD}ATTGGGTTATTAT)-3′: MALDI-TOF [(M − H)$^-$] calcd 9060.89, found 9059.34. 5′-d(ATTTATAGTGTGGGTT^{BD}A^{BD}-ATTGGGTTATTAT)-3′: MALDI-TOF [(M − H)$^-$] calcd 9424.17, found 9425.89. 5′-d(ATTTATAGTGTGGGTT^{BD}A^{BD}A^{BD}ATTGGG-TTATTAT)-3′: MALDI-TOF [(M − H)$^-$] calcd 9786.45, found 9788.19. 5′-d(ATTTATAGTGTGGGTT^{BD}A$_{10}$TTGGGTTATTAT)-3′: MALDI-TOF [(M − H)$^-$] calcd 12 322.39, found 12 322.50. 5′-d(ATTTATAGTGTGGGTT^{BD}A$_{20}$TTGGGTTATTAT)-3′: PAGE purification. 5′-d(ATTTATAGTGTGGGTT^{MD}ATTGGGTTATTAT)-3′: MALDI-TOF [(M − H)$^-$] calcd 9091.92, found 9093.31. 5′-d(ATT-TATAGTGTGGGTT^{MD}A^{MD}ATTGGGTTATTAT)-3′: MALDI-TOF [(M − H)$^-$] calcd 9484.22, found 9482.20. 5′-d(ATTTATAGTGT-GGGTTNDATTGGGTTATTAT)-3′: MALDI-TOF [(M − H)$^-$] calcd 9111.95, found 9112.59. 5′-d(ATTTATAGTGTGGGTTNDANDAT-TGGGTTATTAT)-3′: MALDI-TOF [(M − H)$^-$] calcd 9524.29, found 9524.74. 5′-d(ATTTATAGTGTGGG^{MD}A$_{20}$TGGGTTATTAT)-3′: ESI-TOF [(M − 9H)$^{9-}$] calcd 1773.4693, found 1773.4647.

Measurement of Cyclic Voltammetry (CV) Spectra. Oxidation potentials (E_p) of nucleosides (saturated in water, ca. 200 μM) were measured with an ALS electrochemical analyzer model 660-A in 100 mM LiClO$_4$ solution at room temperature. The scan rate was 100 mV/s. The working electrode was glassy carbon. The counter electrode was Pt wire. The reference electrode was SCE.

Calculation of Stacking Surface Area of Adenine and ^{BD}A Analogues. The interior X_2/T_2 of the duplex 5′-d(AA**XXXX**AA)-3′/5′-d(TTTTTTTT)-3′, as calculated by AMBER* (water set) in MacroModel 6.0, was used for calculating the stacking surface area of X_2/T_2 (R = H in Table 1). The stacking surface area was calculated from (stacking surface area of X_2/T_2) = {(water-accessible surface area of X/T) × 2 − (water-accessible surface area of X_2/T_2)}/2. A probe radius value of 1.4 was used for calculating the water-accessible surface area.

Preparation of ^{32}P-5′-End-labeled Oligomers. The ODNs (400 pmol-strand) were 5′-end-labeled by phosphorylation with 4 μL of [γ-^{32}P]ATP (Amersham) and T4 polynucleotide kinase using a standard procedure. The 5′-end-labeled ODN was recovered by ethanol precipitation and further purified by 15% denaturing polyacrylamide gel electrophoresis (PAGE) and isolated by the crush and soak method.

Hole Transport Experiment and PAGE Analysis. ^{32}P-5′-End-labeled ODNs were hybridized to the complementary strand containing cyanobenzophenone-substituted uridine in 10 mM sodium cacodylate buffer (pH 7.0). Hybridization was achieved by heating the sample at 90 °C for 3 min and slowly cooling to room temperature. Photoirradiation was then carried out in a 100 μL total volume containing 30 kcpm of ^{32}P-5′-end-labeled ODNs and their complementary strands (2 μM strand concentration) in 10 mM sodium cacodylate buffer at pH 7.0. The reaction mixtures were irradiated with a transilluminator (312 nm) at a distance of 3 cm at 0 °C for 45 min. After irradiation, all reaction mixtures were precipitated with the addition of 10 μL of 3 M sodium acetate, 20 μL of herring sperm DNA (50 μM base pair concentration), and 800 μL of ethanol.

The precipitated ODN was washed with 100 μL of 80% cold ethanol and dried in vacuo. The precipitated ODN was resolved in 50 μL of 10% aniline (v/v), heated at 50 °C for 20 min, evaporated by vacuum rotary evaporation to dryness, and resuspended in 5−20 μL of 80% formamide loading buffer (a solution of 80% v/v formamide, 1 mM EDTA, 0.1% xylenecyanol, and 0.1% bromophenol blue). All reactions, along with Maxam−Gilbert G + A sequencing reactions, were conducted with heating at 90 °C for 1 min and quickly chilled on ice. The samples (1 μL, 3−10 kcpm) were loaded onto 15% denaturing 19:1 acrylamide:bisacrylamide gel containing 7 M urea, electrophoresed at 1900 V for approximately 1.5 h, and transferred to a cassette and stored at −80 °C with Fuji X-ray film.

Enzymatic Digestion of ODN after Photoirradiation. An aliquot of photoirradiated ODN solution was fully digested with calf intestine alkaline phosphatase (50 U/mL), snake venom phosphodiesterase (0.15 U/mL), and P1 nuclease (50 U/mL) at 37 °C for 3 h. The digested

solution was analyzed by HPLC on a CHEMCOBOND 5-ODS-H column (4.6 × 150 mm, elution with a solvent mixture of 0.1 M triethylammonium acetate (TEAA), pH 7.0, linear gradient, 0−20% acetonitrile over 10 min, and then 20−80% over another 10 min at a flow rate 1.0 mL/min). The decomposition of nucleosides was determined by the decrease of peak areas of each nucleoside.

Supporting Information Available: Experimental procedures for the synthesis of NDA and the analytical data for enzymatic digestion of ODN after photoirradiation (PDF). This material is available free of charge via the Internet at http://pubs.acs.org.

JA0294008